Transonic Performance of an Auxiliary Airflow System for Axisymmetric Inlets

Norman E. Sorensen* and Eldon A. Latham†
NASA Ames Research Center, Moffett Field, Calif.

A large-scale model of an axisymmetric inlet with a centerbody auxiliary airflow system has been tested in the wind tunnel at transonic speeds. The auxiliary system allows additional airflow (other than in the main duct formed by the cowl and translating centerbody) to pass through the centerbody of the inlet and combine with the main duct airflow on its way to the engine face. The results of the tests are presented, and the inlet performance is compared to a closely related alternative inlet with a "traveling" boundary-layer bleed system that precludes the use of a centerbody auxiliary airflow system. The comparison shows that the auxiliary airflow inlet can supply 7.7% more engine face airflow at Mach number 1.0 and is 26% shorter than the traveling bleed inlet. Even though maximum transonic airflow was not achieved at a comparable engine face mass-flow ratio of 0.580, a total-pressure distortion of 0.10, and a total-pressure recovery of 0.985 were achieved for the auxiliary airflow inlet, whereas a recovery of only 0.965 was achieved for the traveling bleed inlet.

Nomenclature

A_{aux} = area of auxiliary airflow entrance annulus
A_c = cowl-lip area (capture area)
A_o = freestream tube area entering the inlet
D = cowl lip diameter
M_{des} = design Mach number
M_{th} = throat Mach number
M_∞ = freestream Mach number
p_t = total pressure
$\bar{p}_{t_{aux}}$ = average auxiliary duct airflow total pressure at the auxiliary duct exit
$\bar{p}_{t_{main}}$ = average main duct airflow total pressure at the auxiliary duct exit
$p_{t_{2max}}$ = maximum engine face total pressure
$p_{t_{2min}}$ = minimum engine face total pressure
$\bar{p}_{t_2}$ = area-weighted averaged engine face total pressure
$\bar{p}_{t_{2R}}$ = ring average total pressure
p_{t_∞} = freestream total pressure
R_L = cowl lip radius
r = inlet radius
α = angle of attack

Subscripts

aux = auxiliary
main = main duct
R = ring average
2 = engine face

Introduction

ONE of the most likely engine inlet candidates for long-range supersonic cruise aircraft is an axisymmetric mixed-compression inlet system. This type of inlet offers high internal performance over the complete operating Mach number range with a minimum of weight and integrated drag. However, to achieve a reasonable transonic airflow capability while maintaining high internal performance with minimum weight and drag, some form of variable geometry in addition to the translating centerbody must be used. One likely form is an auxiliary airflow system that allows additional airflow to pass through the centerbody of the inlet and combine with the main duct airflow on its way to the engine face. Recently, a large-scale model of an axisymmetric inlet with such a centerbody auxiliary airflow system was tested at transonic speeds in the wind tunnel. The purpose of this paper is to present the results of the test and compare the performance of this inlet to that of a closely related alternative inlet with a "traveling" boundary-layer bleed system, which precludes the use of a centerbody auxiliary airflow system.

Auxiliary Airflow Inlet

The recently tested axisymmetric inlet with a centerbody auxiliary airflow system, called the NASA P_2 inlet, is shown in Fig. 1.[1,2] The inlet is a Mach 2.65 design with a 20-in. capture diameter. The figure shows the inlet with the aft part of the centerbody translated forward to the transonic operating position and the cone forebody translated fully aft forming an auxiliary annulus.[‡]

The annulus lip is the minimum area (throat) and is 10.7% of the cowl lip area. The auxiliary airflow exit is sized so that the two-dimensionally calculated static pressure matches that of the main duct at the exit station. The throat remains fixed on the centerbody as the centerbody translates for off-design supersonic operation. Consequently, no traveling bleed system is required within the centerbody as it is for the alternative inlet to be presented next. Furthermore, the centerbody support struts can penetrate the aft centerbody skirt without disturbing the bleed system at the design centerbody position, resulting in an inlet only 1.63 cowl-lip diameters long measured from the cowl lip to the engine face.

Traveling Bleed Inlet

Without an auxiliary airflow system, only the main duct airflow is available at transonic speeds. An alternative inlet,[3-5] designed to maximize the main duct flow, uses a traveling bleed system. Such an inlet, designated the NASA P inlet, is shown in Fig. 2.

For this type of inlet, the centerbody diameter is less than that for the auxiliary airflow inlet and results in a throat that remains fixed on the cowl rather than on the centerbody.

Presented as Paper 77-148 at the AIAA 15th Aerospace Sciences Meeting, Los Angeles, Calif., Jan. 24-26, 1977; submitted Feb. 3, 1977; revision received July 19, 1977.

Index categories: Airbreathing Propulsion; Transonic Flow.

*Research Scientist. Member AIAA.

†Research Scientist.

‡Since all supersonic mixed-compression inlet systems require boundary-layer bleed systems (not shown) to prevent boundary-layer separation in the supersonic diffuser during started operation, a rather complex multiple cross-passageway system was simulated between the auxiliary airflow passageway and the bleed airflow passageway. This complexity limits the auxiliary airflow area to a maximum of approximately 10-12% of the cowl lip area.

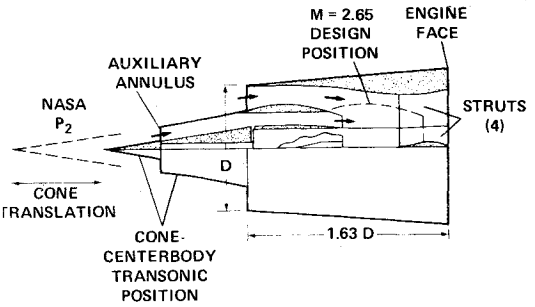

Fig. 1 Auxiliary airflow inlet, $M_{des} = 2.65$.

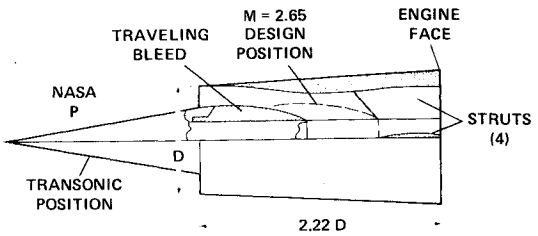

Fig. 2 Traveling bleed inlet, $M_{des} = 2.65$.

Then, to maintain throat bleed opposite the cowl bleed as the centerbody translates for off-design operation, a traveling bleed system is required. This precludes penetration of the struts into the aft centerbody skirt at the design centerbody position and results in a substantially longer inlet at 2.22 lip diameters.

Transonic Airflow Capability

Comparison of the transonic airflow capability of both inlets reveals the improved capability of the auxiliary airflow system. Figure 3 compares the inlet supply mass-flow ratio, A_o/A_c, as a function of Mach number from 0.6 to 1.6, after which the inlets are assumed to start and operate as mixed-compression supersonic inlets. Assuming throat Mach numbers of 0.85, the NASA P_2 inlet has the lowest A_o/A_c ratio when the auxiliary system is closed, $A_{aux}/A_c = 0$, because the maximum centerbody diameter is larger than that of the NASA P inlet. This is a result of fixing the throat on the centerbody in the P_2 inlet. However, with the auxiliary system fully open, $A_{aux}/A_c = 0.107$, the P_2 inlet has a mass-flow ratio 0.04 greater at Mach number 1.0 than the P inlet. The NASA P_2 inlet now matches the airflow demand of a typical afterburning turbojet, the GE4-J5P.

Auxiliary Airflow Inlet Performance

The test results for the NASA P inlet have been presented before.[3-5] The new transonic test results for the NASA P_2 inlet will be presented mainly at $M_\infty = 0.9$. Although the P_2 inlet was not tested at supersonic speed with an operating boundary-layer bleed system, a qualitative assessment of the performance of the subsonic diffuser was made at $M_\infty = 0.90$. This was done by operating the inlet with the centerbody in the design Mach number ($M_{des} = 2.65$) position (see Fig. 1) and with throat Mach numbers simulating the Mach number downstream of a terminal shockwave in the throat. Figure 4 shows such performance where engine face total-pressure recovery, $\bar{p}_{t_2}/p_{t_\infty}$, and total-pressure distortion $(p_{t_{2_{max}}} - p_{t_{2_{min}}})/\bar{p}_{t_2}$ are plotted as a function of throat Mach number M_{th}. At $M_{th} = 0.80$ (Mach number behind a Mach 1.25 terminal shockwave) with only centerbody vortex generators to control distortion at the engine face, the recovery was 0.965, and the distortion was 0.110. Adding vortex generators on the cowl decreased the recovery by 0.020 and increased the distortion by 0.020. Consequently, the rest of the transonic testing was done with only centerbody vortex generators in

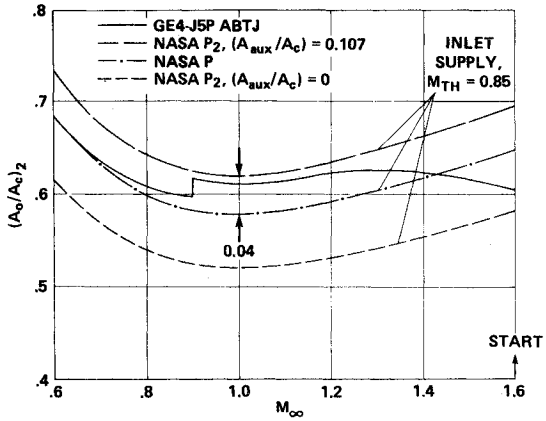

Fig. 3 Transonic airflow capability.

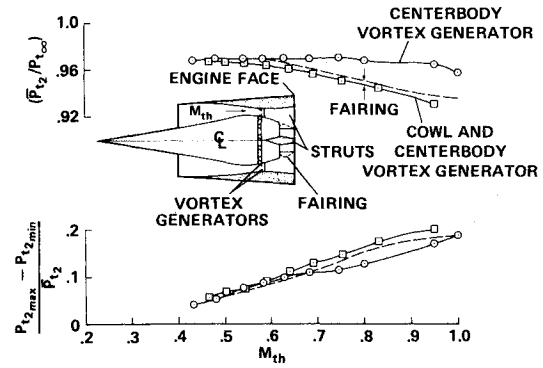

Fig. 4 Design performace at $M_\infty = 0.9$, $\alpha = 0$.

place. Since there is a considerable step between the aft end of the centerbody skirt and the centerbody support tube, a fairing was installed as shown in Fig. 4 to help the flow bridge the step. The beneficial effect of the fairing is apparent, increasing the recovery by approximately 0.005 and decreasing the distortion by approximately 0.02. However, in the test results that follow with the centerbody in the transonic operating position, the fairing was removed[§] since it caused a considerable blockage and reduction in performance at the engine face.

A perspective of the airflow capability of the inlet as the foward spike is translated from closed to fully open, $A_{aux}/A_c = 0.107$, is provided by Fig. 5. Main duct mass-flow ratio, $(A_o/A_c)_{main}$, is plotted as a function of the total mass-flow ratio at the engine face, $(A_o/A_c)_2$, at Mach number 0.90. At the closed position, $A_{aux}/A_c = 0$, the main duct mass-flow ratio, of course, equals the engine face mass-flow ratio. At the fully open position, $A_{aux}/A_c = 0.107$, if the main duct could have been choked simultaneously with the auxiliary duct (the auxiliary duct was choked or nearly choked as will be shown later), the maximum $(A_o/A_c)_2$ ratio would have been approximately 0.64. However, the area distribution in the inlet was such that a minimum area existed in the strut region (downstream of the auxiliary flow duct exit) so that only $(A_o/A_c)_2 = 0.58$ could be achieved.[¶] At the intermediate spike position, $A_{aux}/A_c = 0.053$, the maximum $(A_o/A_c)_2$ ratio was nearly achieved.

As mentioned previously, the auxiliary duct was choked or nearly choked at maximum achievable $(A_o/A_c)_2$ ratio. This is shown in Fig. 6 where auxiliary mass-flow ratio $(A_o/A_c)_{aux}$ is

[§] In a real inlet, the fairing could be mechanically collapsed. Also, hopefully, some mechanical scheme can be designed that would allow the fairing to follow the exit as the centerbody translates forward for started off-design operation.

[¶] A slight increase in the inlet duct length would allow design of narrower struts that would eliminate this problem.

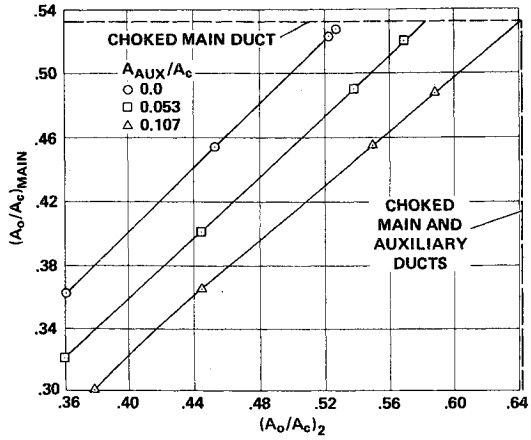

Fig. 5 Airflow capability at $M_\infty = 0.9$, $\alpha = 0$.

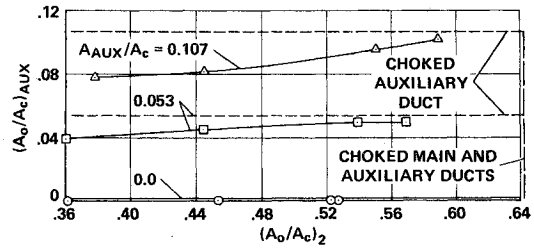

Fig. 6 Auxiliary airflow capability at $M_\infty = 0.9$, $\alpha = 0$.

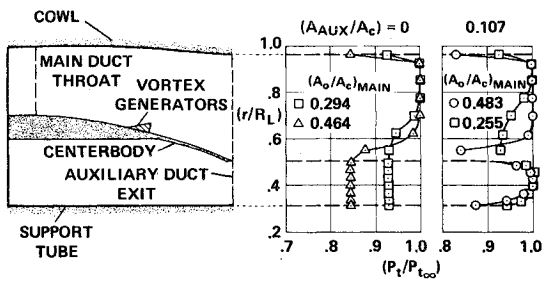

Fig. 7 Profiles at auxiliary duct exit at $M_\infty = 0.9$, $\alpha = 0$.

plotted as a function of $(A_0/A_c)_2$ for the same A_{aux}/A_c as in Fig. 5. With the spike in the closed postion, $(A_o/A_c)_{aux}$ is, of course, 0. At the intermediate position, $(A_o/A_c)_{aux}$ is nearly flat up to maximum $(A_o/A_c)_2$, indicating a choked condition. At the fully open position, the $(A_o/A_c)_{aux}$ ratio approaches choking only at maximum $(A_o/A_c)_2$. Thus, although the main and auxiliary ducts may not choke simultaneously at the maximum engine face mass-flow ratio, the auxiliary duct is capable of providing its full share of the transonic engine face mass flow.

Main and auxiliary duct total-pressure profiles at the auxiliary duct exit station show the condition of both flows before they merge and enter the strut region of the subsonic diffuser. This is shown in Fig. 7 where profiles are plotted for the auxiliary duct closed ($A_{aux}/A_c = 0$) and fully open ($A_{aux}/A_c = 0.107$) for two main duct mass-flow ratios, $(A_o/A_c)_{main}$. With the auxiliary duct closed, the profile is merely a measure of the static pressure at the exit. With the auxiliary duct fully open, the profile is similar to a parabolic pipe flow profile for either main duct mass-flow ratios. For the lower $(A_o/A_c)_{main}$, the profile has low pressure recovery across approximately half of the main duct on the centerbody side, indicating separation of the flow far upstream ahead of the throat.**

**Total-pressure profiles in the thorat indicate upstream separation at the lower main duct mass-flow ratios.[1]

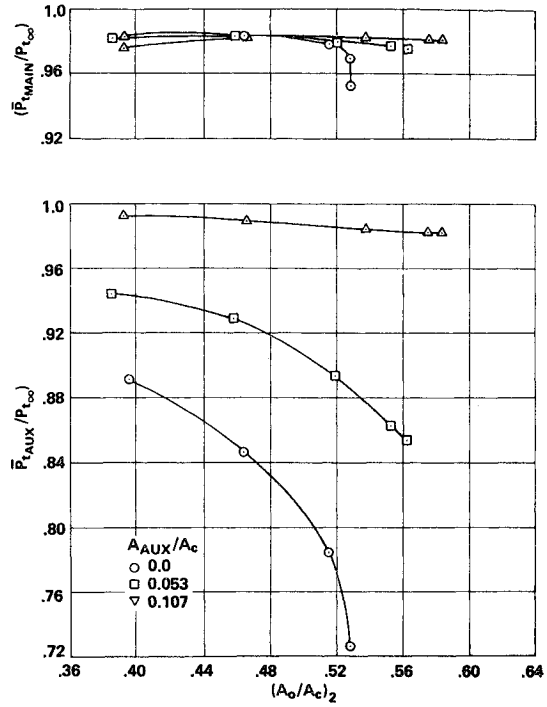

Fig. 8 Recovery at auxiliary duct exit at $M_\infty = 0.9$, $\alpha = 0$.

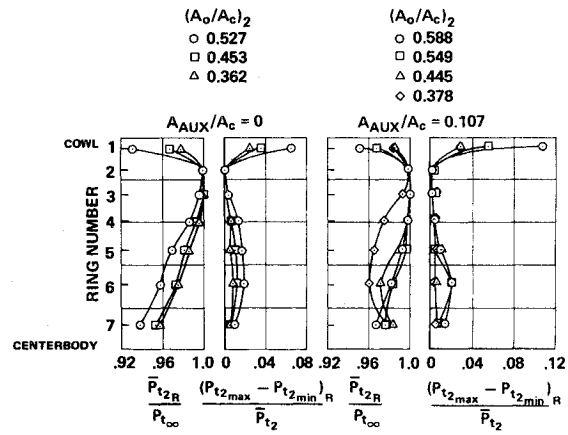

Fig. 9 Engine face profiles at $M_\infty = 0.9$, $\alpha = 0$.

When the main duct flow is increased, the flow remains attached further downstream with separated flow, indicated by the tube nearest the centerbody. However, even with parabolic and separated profiles, the average total-pressure recovery at the auxiliary exit station can be high. The average main and auxiliary duct total-pressure recoveries are plotted in Fig. 8 as a function of the engine face mass-flow ratio for closed, intermediate, and fully open auxiliary duct positions. The main duct recovery remains high at approximately 0.98 over the engine mass-flow range tested except when the main duct flow becomes supercritical with the auxiliary duct closed. The auxiliary duct recovery acts differently, of course, because when closed. the recovery is merely a measure of the static pressure at the base of the centerbody; when at the intermediate duct opening, the recovery decreases as the mass-flow ratio increases because the flow becomes increasingly supercritical (see Fig. 6); when the duct is fully open, the recovery remains high at above 0.98 because the duct flow does not become supercritical.

Further downstream, the total-pressure recovery and distortion profiles reveal the condition of the flow at the engine face and are shown in Fig. 9. The profiles of ring (circumferential) average total-pressure recovery, $\bar{p}_{t_{2_R}}/p_{t_\infty}$,

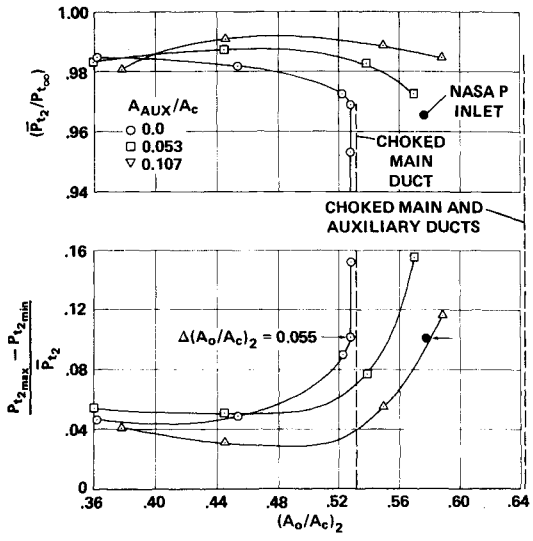

Fig. 10 Engine face performance at $M_\infty = 0.9$, $\alpha = 0$.

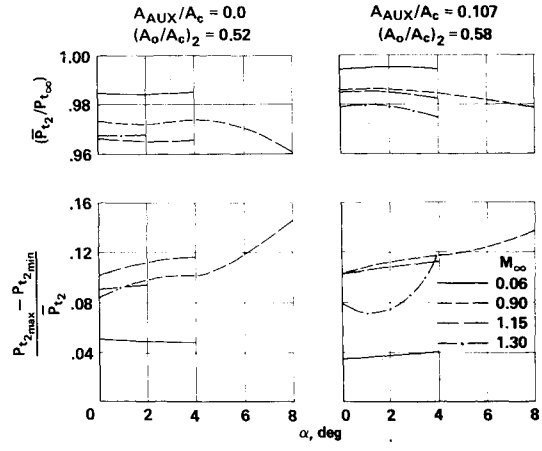

Fig. 11 Performance at angle of attack.

and distortion, $(p_{t_{2_{max}}} - p_{t_{2_{min}}})_R / p_{t_2}$, at seven radial stations are plotted for the auxiliary duct closed and fully open and for several engine face mass-flow ratios. With the auxiliary duct closed, the main duct flow expands suddenly off of the centerbody skirt at the auxiliary duct exit, contributing to the relatively low recovery across approximately half of the support-tube side of the duct. With the auxiliary duct fully open, the auxiliary base is filled with airflow and contributes to the generally higher recovery across the engine face. In either case, the ring distortion nearest the cowl is highest because one quadrant of the flow has low performance[1] for as yet undetermined reasons. If the low-performance quadrant were ignored, the distortion would be reduced significantly.

The overall performance at the engine face is shown in Fig. 10. Total-pressure recovery and distortion are plotted as a function of engine face mass-flow ratio for closed, intermediate, and fully open auxiliary duct openings. As the auxiliary duct is opened, the recovery increases and the distortion decreases, as would be expected from the profiles in Fig. 9. As mentioned previously, the full potential engine face mass-flow ratio could not be achieved because the internal area distribution of the inlet caused choking in the strut region before the main duct choked. Even so, with a distortion of 0.10, the mass-flow ratio was increased from 0.525 to 0.580 with a high-pressure recovery of 0.985. At nearly comparable conditions, the NASA P inlet provided only 0.965 recovery with 0.10 distortion. Furthermore, without the low-performance quadrant, as mentioned earlier, at $(A_o/A_c)_2 = 0.588$ the distortion would be reduced from 0.12 to 0.05 with a slight increase in recovery from 0.984 to 0.986. Consequently, without choking at the struts and without one low-performance quadrant, it is believed that the maximum potential engine face mass-flow ratio of 0.64 with high performance can be achieved for the NASA P_2 inlet system.

The inlet has also maintained high performance at angle of attack as shown in Fig. 11. Engine face total-pressure recovery and distortion are plotted as a function of angles of attack up to 8 deg for the auxiliary duct closed and fully open and for nearly maximum mass-flow ratio, $(A_o/A_c)_2 = 0.52$ and 0.58, respectively. Data are also presented for a range of Mach numbers from 0.6 to 1.3. Up to 4-deg angle of attack, the inlet performed well with the distortion varying approximately from 0.04 to 0.12, and the recovery remaining nearly constant at each Mach number and never less than 0.965.

Concluding Remarks

Comparison of the auxiliary airflow inlet with a closely related alternative inlet equipped with a traveling bleed system has shown that the auxiliary airflow inlet can supply 7.7% more engine face airflow at Mach 1.0. In addition, the auxiliary airflow inlet is 26.6% shorter than the traveling bleed inlet. Even though the auxiliary airflow inlet as tested choked prematurely in the centerbody support strut region, it is believed that modification of the strut region would eliminate choking and yield better transonic performance with a maximum potential engine face airflow greater than that of the traveling bleed inlet.

References

[1] Santman, D.M., "Transonic Performance of a Mach 2.65 Auxiliary Flow Axisymmetric Inlet," NASA CR-2747, June 1976.

[2] Sorensen, N.E., Latham, E.A., and Smeltzer, D.B., "Variable Geometry for Supersonic Mixed-Compression Inlets," *Journal of Aircraft*, Vol. 13, April 1976, pp. 309-312.

[3] Smeltzer, D.B. and Sorensen, N.E., "Analytical and Experimental Performance of Two Isentropic Mixed Compression Axisymmetric Inlets at Mach Numbers 0.8 to 2.65," NASA TN D-7320, June 1973.

[4] Smeltzer, D.B. and Sorensen, N.E., "Tests of a Mixed Compression Axisymmetric Inlet with Large Transonic Mass Flow at Mach Numbers 0.6 to 2.65," NASA TN D-6971, Dec. 1972.

[5] Koncsek, J.L. and Syberg, J., "Transonic and Supersonic Test of a Mach 2.65 Mixed-Compression Axisymmetric Intake," NASA CR-1977, March 1972.